ELSEVIER

Journal of Computational and Applied Mathematics 145 (2002) 189–211

JOURNAL OF COMPUTATIONAL AND APPLIED MATHEMATICS

www.elsevier.com/locate/cam

Parallel Schwarz methods for convection-dominated semilinear diffusion problems

V. Sirotkin[a,*], P. Tarvainen[b,1]

[a] *Institute of Microelectronics Technology, Russian Academy of Sciences, Moscow District, 142432 Chernogolovka, Russia*

[b] *Department of Mathematical Information Technology, University of Jyväskylä, P.O. Box 35, FIN-40351 Jyväskylä, Finland*

Received 7 October 2000; received in revised form 25 August 2001

Abstract

Parallel two-level Schwarz methods are proposed for the numerical solution of convection-diffusion problems, with the emphasis on convection-dominated problems. Two variants of the methodology are investigated. They differ from each other by the type of boundary conditions (Dirichlet- or Neumann-type) posed on a part of the second-level subdomain interfaces. Convergence properties of the two-level Schwarz methods are experimentally compared with those of a variant of the standard multi-domain Schwarz alternating method. Numerical experiments performed on a distributed memory multiprocessor computer illustrate parallel efficiency of the methods. © 2001 Elsevier Science B.V. All rights reserved.

MSC: 35B25; 65N55; 65Y05

Keywords: Singularly perturbed semilinear convection–diffusion problem; Multi-level Schwarz methods; Parallel computing

1. Introduction

We are interested in parallel algorithms based on overlapping domain decomposition for the numerical solution of singularly perturbed semilinear elliptic problems of the form

$$\begin{aligned} &\mathscr{L}u(P) = \varepsilon\Delta u(P) + \mathbf{b}(P)\cdot\nabla u(P) = f(P,u),\ P=(x,y)\in\Omega,\\ &u(P) = U(P), \qquad\qquad P\in\partial\Omega, \end{aligned} \tag{1}$$

* Corresponding author.

E-mail addresses: sirotkin@ipmt-hpm.ac.ru (V. Sirotkin), pasi.tarvainen@numerola.fi (P. Tarvainen).

[1] Present address: Numerola Oy (Ltd), Väinönkatu 11A, FIN-40100 Jyväskylä, Finland.

0377-0427/01/$ - see front matter © 2001 Elsevier Science B.V. All rights reserved.
PII: S0377-0427(01)00575-1

posed on a bounded domain $\Omega \subset \mathbb{R}^2$, where ε is a positive parameter, the diffusion coefficient, $\mathbf{b}(P) = (b^x(P), b^y(P))$ is a vector field representing the convection, and $\partial\Omega$ denotes the boundary of the domain Ω. The functions $b^x(P)$, $b^y(P)$, $f(P,u)$, and $U(P)$ are assumed to be sufficiently smooth with f satisfying $f_u(P,u) = (\partial/\partial u) f(P,u) \geqslant 0$. Under suitable continuity and compatibility conditions on the data, a unique solution $u(P)$ of the problem (1) exists (see [12] for details). Furthermore, for $\varepsilon \ll 1$, the problem is singularly perturbed and has boundary layers of width $\mathcal{O}(\varepsilon)$ according to the boundary conditions and the convection vector (see, e.g., [3,15]).

Convection-dominated semilinear equations of the form (1) frequently occur in mathematical models of physical and chemical processes. Well-known application fields are the heat-conduction [1] and convection–diffusion reaction equations [20] with nonlinear sources. In addition, mention may be made of the following application areas: counterflow flames modelling [9,17,18] and semiconductor device simulation based on the so-called drift-diffusion model [23]. Implementation of domain decomposition methods allows to construct efficient numerical algorithms on massively parallel computers for such problems.

In [4,24], the parallel two-level Schwarz method was proposed. This domain decomposition method is based on the classical Schwarz alternating procedure [22] and can be regarded as an additive process with second-level (interface) problems. The modification of the method, where the Dirichlet boundary conditions on a part of the second-level subdomain interfaces are replaced by the Neumann boundary conditions, has a better convergence rate than the original method [25]. Parallel implementation of the above Schwarz methods for singularly perturbed self-adjoint elliptic problems was considered in [27,26]. The goal of this paper is to compare the convergence properties and the parallel efficiency of both two-level Schwarz methods among themselves as well as to a variant of the standard multi-domain Schwarz method in the case of singularly perturbed convection–diffusion problems of the form (1).

We emphasize that the methods from [24,25] can be successfully applied to linearized variants of the problem (1) and similar problems are extensively used as (simplified) model problems for the development and the verification of domain decomposition methods used in computational fluid dynamics, see for example, [5–8,10,11,13,19], and references therein.

The rest of the paper is divided into four sections. In Section 2, we describe the three variants of the Schwarz method. In Section 3, parallel implementation of the methods on distributed memory computer is proposed. The results of the numerical experiments are reported in Section 4. In the last section, some concluding remarks is given.

2. Overlapping Schwarz methods

In this section, the three variants of the Schwarz method for the problem (1) are described and evaluated.

2.1. Domain decomposition and related notations

For simplicity, we consider a rectangular domain $\Omega = (0, X) \times (0, Y)$ as well as rectangular subdomain partitionings. We introduce an *overlapping* multi-domain decomposition of the domain Ω into

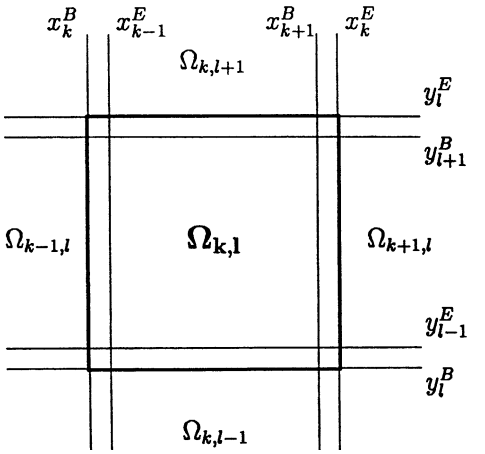


Fig. 1. Fragment of an overlapping multi-domain decomposition of the domain Ω into the subdomains $\Omega_{k,l}$.

$K \times L$ subdomains $\Omega_{k,l}$ as follows (see Fig. 1):

$$\Omega_{k,l} = (x_k^B, x_k^E) \times (y_l^B, y_l^E), \quad 1 \leqslant k \leqslant K, \quad 1 \leqslant l \leqslant L,$$

where

$$0 < x_k^B < x_{k-1}^E < x_{k+1}^B < x_k^E < X, \quad 2 \leqslant k \leqslant K-1, \quad x_1^B = 0, \quad x_K^E = X,$$
$$0 < y_l^B < y_{l-1}^E < y_{l+1}^B < y_l^E < Y, \quad 2 \leqslant l \leqslant L-1, \quad y_1^B = 0, \quad y_L^E = Y.$$

The (minimum) sizes of the overlappings between subdomains $\Omega_{k,l}$ are given by

$$D^x = \min_{1 \leqslant k \leqslant K-1} (x_k^E - x_{k+1}^B), \qquad D^y = \min_{1 \leqslant l \leqslant L-1} (y_l^E - y_{l+1}^B).$$

In the following, we shall use the auxiliary subdomains $\omega_{k,l}$, $1 \leqslant k \leqslant K$, $1 \leqslant l \leqslant L$, defined by

$$\begin{aligned}\omega_{k,l} = (&\{(x,y) : x_k^B < x < x_{k-1}^E,\ y_l^B < y < \sigma(x, x_k^B, x_{k-1}^E, y_{l-1}^E, y_l^B)\} \\ &\cup \{(x,y) : x_k^B < x < x_{k-1}^E,\ \sigma(x, x_k^B, x_{k-1}^E, y_{l+1}^B, y_l^E) < y < y_l^E\} \\ &\cup \{(x,y) : x_{k+1}^B < x < x_k^E,\ \sigma(x, x_{k+1}^B, x_k^E, y_l^E, y_{l+1}^B) < y < y_l^E\} \\ &\cup \{(x,y) :\ x_{k+1}^B < x < x_k^E,\ y_l^B < y < \sigma(x, x_{k+1}^B, x_k^E, y_l^B, y_{l-1}^E)\}),\end{aligned}$$

where σ is a linear interpolant defined by

$$\sigma(r, r_1, r_2, s_1, s_2) = \frac{s_1(r_2 - r) + s_2(r - r_1)}{r_2 - r_1},$$

with $x_0^E \equiv 0$, $x_{K+1}^B \equiv X$, $y_0^E \equiv 0$, and $y_{L+1}^B \equiv Y$.

Furthermore, for the two-level Schwarz methods (Sections 2.3.1 and 2.3.2), we introduce a *nonoverlapping* multi-domain decomposition of the domain Ω into $K \times L$ subdomains $\Theta_{k,l}$, the

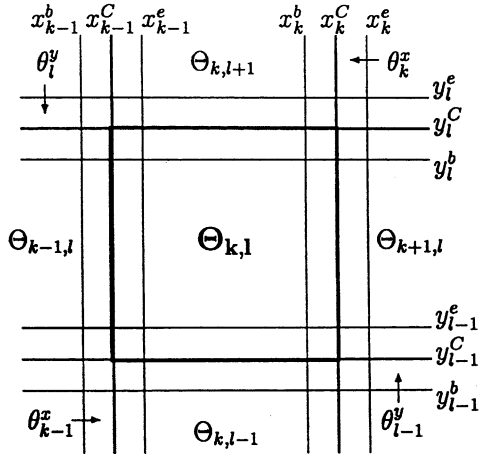


Fig. 2. Fragment of two-level partitionings of the domain Ω: *first-level* subdomains $\Theta_{k,l}$ and *second-level* subdomains θ^x_k and θ^y_l.

first-level subdomains, by (see Fig. 2):

$$\Theta_{k,l} = (x^C_{k-1}, x^C_k) \times (y^C_{l-1}, y^C_l), \quad 1 \leqslant k \leqslant K,\ 1 \leqslant l \leqslant L,$$

where

$$0 < x^C_{k-1} < x^C_k < X, \quad 2 \leqslant k \leqslant K-1, \quad x^C_0 = 0, \quad x^C_K = X,$$
$$0 < y^C_{l-1} < y^C_l < Y, \quad 2 \leqslant l \leqslant L-1, \quad y^C_1 = 0, \quad y^C_L = Y.$$

We also define sets $\{\theta^x_k\}$ and $\{\theta^y_l\}$ of interface subdomains, the *second-level* subdomains, by

$$\theta^x_k = (x^b_k, x^e_k) \times (0, Y), \quad 0 < x^b_k < x^C_k < x^e_k < X,\ 1 \leqslant k \leqslant K-1, \quad \Theta^x = \bigcup_{k=1}^{K-1} \theta^x_k,$$

$$\theta^y_l = (0, X) \times (y^b_l, y^e_l), \quad 0 < y^b_l < y^C_l < y^e_l < Y,\ 1 \leqslant l \leqslant L-1, \quad \Theta^y = \bigcup_{l=1}^{L-1} \theta^y_l.$$

The overlapping interval sizes of the first-level and second-level subdomains are determined by the following parameters:

$$d^x = \min_{1 \leqslant k \leqslant K-1} \{\min[(x^C_k - x^b_k), (x^e_k - x^C_{k+1})]\}, \quad d^y = \min_{1 \leqslant l \leqslant L-1} \{\min[(y^C_l - y^b_l), (y^e_l - y^C_{l+1})]\}.$$

Finally, we determine the boundaries of θ^x_k, $1 \leqslant k \leqslant K-1$, and θ^y_l, $1 \leqslant l \leqslant L-1$, by

$$\overset{x}{\gamma}{}^b_k = \{(x, y) : x = x^b_k,\ 0 < y < Y\}, \quad \overset{x}{\gamma}{}^e_k = \{(x, y) : x = x^e_k,\ 0 < y < Y\};$$

$$\overset{y}{\gamma}{}^l_k = \{(x, y) : 0 < x < X,\ y = y^b_l\}, \quad \overset{y}{\gamma}{}^e_l = \{(x, y) : 0 < x < X,\ y = y^e_l\}.$$

2.2. Multi-domain Schwarz alternating method

Using the above described domain partitioning, we can introduce a parallel version of the Schwarz alternating method based on an odd–even ordering of the subdomains $\Omega_{k,l}$, $1 \leqslant k \leqslant K$, $1 \leqslant l \leqslant L$:

$$\Omega_{\text{odd}} = \bigcup_{(k,l)\in\mathscr{S}_{\text{odd}}} \Omega_{k,l}, \quad \mathscr{S}_{\text{odd}} = \{(k,l) : k + l \text{ odd}\};$$

$$\Omega_{\text{even}} = \bigcup_{(k,l)\in\mathscr{S}_{\text{even}}} \Omega_{k,l}, \quad \mathscr{S}_{\text{even}} = \{(k,l) : k + l \text{ even}\}.$$

The multi-domain Schwarz alternating method

Step 0: Initialization: choose an initial function $V^0_{\text{odd}}(P)$, $P \in \Omega_{\text{odd}}$.

Step 1: Solve *simultaneously* the subproblems on the "*even*" subdomains:

$$\begin{aligned} &\mathscr{L} v^n_{k,l}(P) = f(P, v^n_{k,l}), && P \in \Omega_{k,l}, \quad (k,l) \in \mathscr{S}_{\text{even}}, \\ &v^n_{k,l}(P) = U(P), && P \in \partial\Omega_{k,l} \cap \partial\Omega, \\ &v^n_{k,l}(P) = V^{n-1}_{\text{odd}}(P), && P \in \partial\Omega_{k,l} \setminus \partial\Omega, \end{aligned} \tag{2}$$

where

$$V^n_{\text{odd}}(P) = v^n_{k,l}(P), \quad P \in \begin{cases} \Omega_{k,l} \setminus \bar{\omega}_{k,l}, \ (k,l) \in \mathscr{S}_{\text{odd}}, \\ \Omega_{k,l} \setminus \omega_{k,l}, \ (k,l) \in \mathscr{S}_{\text{odd}} \cap \{k \text{ odd}\}. \end{cases}$$

Step 2: Solve *simultaneously* the subproblems on the "*odd*" subdomains:

$$\begin{aligned} &\mathscr{L} v^n_{k,l}(P) = f(P, v^n_{k,l}), && P \in \Omega_{k,l}, \quad (k,l) \in \mathscr{S}_{\text{odd}}, \\ &v^n_{k,l}(P) = U(P), && P \in \partial\Omega_{k,l} \cap \partial\Omega, \\ &v^n_{k,l}(P) = V^{n}_{\text{even}}(P), && P \in \partial\Omega_{k,l} \setminus \partial\Omega, \end{aligned} \tag{3}$$

where

$$V^n_{\text{even}}(P) = v^n_{k,l}(P), \quad P \in \begin{cases} \Omega_{k,l} \setminus \bar{\omega}_{k,l}, \ (k,l) \in \mathscr{S}_{\text{even}}, \\ \Omega_{k,l} \setminus \omega_{k,l}, \ (k,l) \in \mathscr{S}_{\text{even}} \cap \{k \text{ odd}\}. \end{cases}$$

Step 3: Stopping criterion: if a prescribed accuracy is reached, then stop; otherwise go to Step 1. From now on, the method will be abbreviated by the *mdS-method.*

As the solution at the nth iteration step of the mdS-method, we can take the following function:

$$V^n(P) = \begin{cases} V^n_{\text{even}}, & P \in \Omega_{\text{even}} \setminus \Omega_{\text{odd}}, \\ V^n_{\text{odd}}, & P \in \Omega_{\text{odd}}. \end{cases}$$

Note that at $K > 1$ and $L > 1$ the solution $V^n(P)$ has *discontinuities* of the first kind on the boundaries $\bigcup_{(k,l)\in\mathscr{S}_{\text{odd}}} \overline{(\Omega_{k,l} \setminus \bar{\omega}_{k,l})}$.

Remark 1. The mdS-method consists of two sequential steps but the subproblems within these steps can be solved concurrently. Thus, the method can be realized on $\lfloor \frac{1}{2}(K \times L + 1) \rfloor$ processors, and each of $\lfloor \frac{1}{2}(K \times L) \rfloor$ processors contains a "odd–even" pair of subproblems.

2.3. Two-level Schwarz methods

First we describe the two-level Schwarz methods in a general form. Two variants resulting from this formulation differ from each other by the boundary conditions for the interface subdomains. These variants are presented in the following subsections.

The two-level Schwarz method

Step 0: Initialization: choose initial functions $v^0_{k,l}(P)$, $P \in \bar{\Theta}_{k,l}$, $1 \leqslant k \leqslant K$, $1 \leqslant l \leqslant L$.

Step 1: Solve *simultaneously* the subproblems on the *interface* subdomains θ^x_k, $1 \leqslant k \leqslant K-1$:

$$\begin{aligned}
&\mathscr{L}\overset{x}{w}{}^n_k(P) = f(P, \overset{x}{w}{}^n_k), && P \in \theta^x_k,\\
&\overset{x}{w}{}^n_k(P) = U(P), && P \in \partial\theta^x_k \cap \partial\Omega,\\
&\overset{x\,b}{\mathscr{G}}[\overset{x}{w}{}^n_k(P) - V^{n-1}(P)] = 0, && P \in \overset{x}{\gamma}{}^b_k,\\
&\overset{x\,e}{\mathscr{G}}[\overset{x}{w}{}^n_k(P) - V^{n-1}(P)] = 0, && P \in \overset{x}{\gamma}{}^e_k,
\end{aligned} \tag{4}$$

where

$$V^n(P) = v^n_{k,l}(P),\ P \in \bar{\Theta}_{k,l},\ 1 \leqslant k \leqslant K,\ 1 \leqslant l \leqslant L.$$

Step 2: Solve *simultaneously* the subproblems on the *interface* subdomains θ^y_l, $1 \leqslant l \leqslant L-1$:

$$\begin{aligned}
&\mathscr{L}\overset{y}{w}{}^n_l(P) = f(P, \overset{y}{w}{}^n_l), && P \in \theta^y_l,\\
&\overset{y}{w}{}^n_l(P) = U(P), && P \in \partial\theta^y_l \cap \partial\Omega,\\
&\overset{y\,b}{\mathscr{G}}[\overset{y}{w}{}^n_l(P) - V^{n-1}(P)] = 0, && P \in \overset{y}{\gamma}{}^l_k \setminus \Theta^x,\\
&\overset{y\,b}{\mathscr{G}}[\overset{y}{w}{}^n_l(P) - \overset{x\,n}{W}(P)] = 0, && P \in \overset{y}{\gamma}{}^l_k \cap \Theta^x,\\
&\overset{y\,e}{\mathscr{G}}[\overset{y}{w}{}^n_l(P) - V^{n-1}(P)] = 0, && P \in \overset{y}{\gamma}{}^e_l \setminus \Theta^x,\\
&\overset{y\,e}{\mathscr{G}}[\overset{y}{w}{}^n_l(P) - \overset{x\,n}{W}(P)] = 0, && P \in \overset{y}{\gamma}{}^e_l \cap \Theta^x,
\end{aligned} \tag{5}$$

where

$$\overset{x\,n}{W}(P) = \overset{x}{w}{}^n_k(P), \quad P \in \bar{\theta}^x_k, \quad 1 \leqslant k \leqslant K-1.$$

Step 3: Solve *simultaneously* the subproblems on the *first-level* subdomains $\Theta_{k,l}$, $1 \leqslant k \leqslant K$, $1 \leqslant l \leqslant L$:

$$\begin{aligned}
&\mathscr{L}v^n_{k,l}(P) = f(P, v^n_{k,l}), && P \in \Theta_{k,l},\\
&v^n_{k,l}(P) = U(P), && P \in \partial\Theta_{k,l} \cap \partial\Omega,\\
&v^n_{k,l}(P) = W^n(P), && P \in \partial\Theta_{k,l} \setminus \partial\Omega,
\end{aligned} \tag{6}$$

where

$$W^n(P) = \begin{cases} \overset{x}{W}{}^n(P),\ P \in \bar{\Theta}^x \setminus \bar{\Theta}^y, \\ \overset{y}{W}{}^n(P),\ P \in \bar{\Theta}^y, \end{cases} \quad \overset{y}{W}{}^n(P) = \overset{y}{w}{}_l^n(P),\ P \in \bar{\theta}_l^y,\ 1 \leqslant l \leqslant L-1.$$

Step 4: Stopping criterion: if a prescribed accuracy is reached, then stop; otherwise go to Step 1.

We emphasize that as the solution at the nth iteration step of the proposed method the *continuous* function $V^n(P)$ is taken.

Remark 2. We notice that the two-level Schwarz method involves three sequential steps; however, the subproblems associated with the first-level subdomains in Step 3 can be solved in parallel. The same is true for the interface subproblems in Steps 1 and 2. Hence, we can realize the method on $K \times L$ processors: the subproblems related to the subdomains $\Omega_{k,l}$ are mapped onto individual processors. The second-level subproblems (related to θ_k^x and θ_l^y) are placed into processors containing one of the first-level subproblems.

2.3.1. The DDS-method: the two-level Schwarz method with interface subdomains using "Dirichlet–Dirichlet" scheme

In the case of the *DDS-method*, we suppose $\overset{x}{\mathscr{G}}{}^{b,e} \equiv 1$ and $\overset{y}{\mathscr{G}}{}^{b,e} \equiv 1$ on the boundaries $\overset{x}{\gamma}{}_k^{b,e}$, $1 \leqslant k \leqslant K-1$, and $\overset{y}{\gamma}{}_l^{b,e}$, $1 \leqslant l \leqslant L-1$, respectively, that is, for the interface subproblems from (4) and (5), we apply the boundary conditions of Dirichlet-type only.

2.3.2. The NDS-method: the two-level Schwarz method with interface subdomains using "Neumann–Dirichlet" scheme

In the *NDS-method*, we use boundary conditions of Dirichlet- or Neumann-type depending on the convection. Namely, the operators $\overset{x}{\mathscr{G}}{}^{b,e}$ on the boundaries $\overset{x}{\gamma}{}_k^{b,e}$, $1 \leqslant k \leqslant K-1$ are defined by

$$\overset{x}{\mathscr{G}}{}^{b}[z(x_k^b, y)] = \begin{cases} \left.\dfrac{\partial z(x,y)}{\partial x}\right|_{x=x_k^b}, & b^x(x_k^b, y) \geqslant 0, \\ z(x_k^b, y), & b^x(x_k^b, y) < 0, \end{cases} \qquad 0 < y < Y. \tag{7}$$

$$\overset{x}{\mathscr{G}}{}^{e}[z(x_k^e, y)] = \begin{cases} \left.\dfrac{\partial z(x,y)}{\partial x}\right|_{x=x_k^e}, & b^x(x_k^e, y) \leqslant 0 \ \text{ and } \ b^x(x_k^b, y) < 0, \\ z(x_k^e, y), & \text{otherwise}, \end{cases}$$

The operators $\overset{y}{\mathscr{G}}{}^{b,e}$ on the boundaries $\overset{y}{\gamma}{}_l^{b,e}$, $1 \leqslant l \leqslant L-1$, are defined in similar fashion.

2.4. Convergence results for the Schwarz methods for a model problem

In this section, we present the convergence and the convergence rate of the Schwarz methods for a model problem of the form (1) with a constant transport vector and with a linear

right-hand side:

$$\mathbf{b}(P) = (1, 0), \quad f(P, u) = F(P). \tag{8}$$

Moreover, we here analyse the Schwarz methods in the case of a strip domain decomposition, namely, for the domain partitionings with $L = 1$.

Theorem 1. *If $n \geqslant N_0$ with $N_0 = \lfloor \frac{1}{2}K \rfloor$ for the mdS-method or $N_0 = K - 1$ for the DDS- and NDS-methods then the Schwarz methods converge to the solution $u(P)$ of the model problem* (1), (8) *with linear (geometrical) rate $q \in (0, 1)$, that is,*

$$\|V^n(P) - u(P)\|_\Omega \leqslant q^{n-N_0+1} \|V^0(P) - u(P)\|_\Omega, \quad n \geqslant N_0,$$

where $\|A(P)\|_{\Omega_a} \equiv \max_{P \in \Omega_a} |A(P)|$ and $V^n(P)$ is the solution at the nth iteration step of the corresponding Schwarz method (see Sections 2.2 or 2.3). For the contraction factor q the bound

$$q \leqslant q_0 \exp(-\varepsilon^{-1}\rho),$$

holds, where $\rho = D^x$ for the mdS-method or $\rho = d^x$ for the DDS- and NDS-methods with D^x and d^x being defined in Section 2.1. For q_0 the following relationships are valid: $q_0 = K - 1$ for the mdS- and NDS-methods and $q_0 = 2(K - 1)\exp[-\exp(-\varepsilon^{-1}\rho)\ln(2)]$ for the DDS-method.

The proof technique of the convergence results for the mdS- and DDS-methods will be illustrated in the following subsection by the example of the latter one. The convergence properties for the NDS-method can be easily established, combining the results from Section 2.5 and [25].

2.5. Proof of Theorem 1 for the DDS-method

We first remind that we here prove the convergence result for the DDS-method in the case of a strip first-level domain decomposition with $L = 1$ (i.e., for the variant of the method without Step 2, see Section 2.3) and for the problem (1) with constant convection and the linear right-hand side (8).

Introduce the functions

$$\overset{x}{\xi}{}^n_k(P) = \overset{x}{w}{}^n_k(P) - u(P), \quad 1 \leqslant k \leqslant K - 1,$$

$$\zeta^n_{k,1}(P) = v^n_{k,1}(P) - u(P), \quad 1 \leqslant k \leqslant K.$$

From (4), (6) and (8), at $n \geqslant 1$, we have

$$\begin{aligned} &\mathscr{L}\overset{x}{\xi}{}^n_k(P) = 0, && P \in \theta^x_k, \\ &\overset{x}{\xi}{}^n_k(P) = 0, && P \in \partial\theta^x_k \cap \partial\Omega, \\ &\overset{x}{\xi}{}^n_k(P) = Z^{n-1}(P), && P \in \partial\theta^x_k \setminus \partial\Omega; \end{aligned} \tag{9}$$

and

$$\begin{aligned}
&\mathscr{L}\zeta^n_{k,1}(P) = 0, && P \in \Theta_{k,1},\\
&\zeta^n_{k,1}(P) = 0, && P \in \partial\Theta_{k,1} \cap \partial\Omega,\\
&\zeta^n_{k,1}(P) = \overset{x}{\Xi}{}^n(P), && P \in \partial\Theta_{k,1} \setminus \partial\Omega,
\end{aligned} \tag{10}$$

where

$$Z^n(P) = \zeta^n_{k,1}(P),\ P \in \bar{\Theta}_{k,1},\ 1 \leqslant k \leqslant K, \qquad \overset{x}{\Xi}{}^n(P) = \overset{x}{\xi}{}^n_k(P),\ P \in \bar{\theta}^x_k,\ 1 \leqslant k \leqslant K-1.$$

Consider the following one-dimensional problems:

$$\begin{aligned}
&\varepsilon[\phi^{\mathrm{I,II}}(x,x^s,x^f)]'' + [\phi^{\mathrm{I,II}}(x,x^s,x^f)]' = 0, && x \in (x^s,x^f),\\
&\phi^{\mathrm{I}}(x^s,x^s,x^f) = 1, && \phi^{\mathrm{I}}(x^f,x^s,x^f) = 0,\\
&\phi^{\mathrm{II}}(x^s,x^s,x^f) = 0, && \phi^{\mathrm{II}}(x^f,x^s,x^f) = 1,
\end{aligned} \tag{11}$$

where

$$\phi^{\mathrm{I}}(x,x^s,x^f) = \frac{\exp[-\varepsilon^{-1}(x-x^s)] - \exp[-\varepsilon^{-1}(x^f-x^s)]}{1-\exp[-\varepsilon^{-1}(x^f-x^s)]},$$

$$\phi^{\mathrm{II}}(x,x^s,x^f) = \frac{1-\exp[-\varepsilon^{-1}(x-x^s)]}{1-\exp[-\varepsilon^{-1}(x^f-x^s)]}. \tag{12}$$

According to (9)–(11) and a standard comparison theorem, we can write

$$\begin{aligned}
&|\overset{x}{\xi}{}^n_k(P)|_{P\in\bar{\theta}^x_k} \leqslant \|\overset{x}{\xi}{}^n_k(P)\|_{\overset{x}{\gamma}{}^b_k}\phi^{\mathrm{I}}(x,x^b_k,x^e_k) + \|\overset{x}{\xi}{}^n_k(P)\|_{\overset{x}{\gamma}{}^e_k}\phi^{\mathrm{II}}(x,x^b_k,x^e_k),\\
&|\zeta^n_{k,1}(P)|_{P\in\bar{\Theta}_{k,1}} \leqslant \|\zeta^n_{k,1}(P)\|_{\overset{x}{\gamma}{}^C_{k-1}}\phi^{\mathrm{I}}(x,x^C_{k-1},x^C_k) + \|\zeta^n_{k,1}(P)\|_{\overset{x}{\gamma}{}^C_k}\phi^{\mathrm{II}}(x,x^C_{k-1},x^C_k),
\end{aligned} \tag{13}$$

where

$$\overset{x}{\gamma}{}^C_k = \{(x,y) : x = x^C_k,\ 0 < y < Y\}.$$

Now, denote

$$\delta^n_k = \|\zeta^n_{k,1}(P)\|_{\overset{x}{\gamma}{}^C_k}, \qquad \Delta^n = \max_{1\leqslant k\leqslant K}\delta^n_k, \quad n \leqslant 1.$$

Then, from (10) and the maximum principle, it follows that

$$\max_{1\leqslant k\leqslant K}\|\zeta^n_{k,1}(P)\|_{\bar{\Theta}_{k,1}} \leqslant \Delta^n.$$

From (9), (10) and (13), we get

$$\delta^n_k \leqslant \overset{1}{\psi}_k\delta^{n-1}_{k-1} + \overset{2}{\psi}_k\delta^{n-1}_k + \overset{3}{\psi}_k\delta^{n-1}_{k+1}, \qquad 1 \leqslant k \leqslant K-1, \qquad \delta^n_0 = \delta^n_K = 0,$$

where

$$\overset{1}{\psi}_k = \phi^{\mathrm{I}}(x_k^b, x_{k-1}^C, x_k^C)\phi^{\mathrm{I}}(x_k^C, x_k^b, x_k^e),$$

$$\overset{2}{\psi}_k = \phi^{\mathrm{II}}(x_k^b, x_{k-1}^C, x_k^C)\phi^{\mathrm{I}}(x_k^C, x_k^b, x_k^e) + \phi^{\mathrm{I}}(x_k^e, x_k^C, x_{k+1}^C)\phi^{\mathrm{II}}(x_k^C, x_k^b, x_k^e),$$

$$\overset{3}{\psi}_k = \phi^{\mathrm{II}}(x_k^e, x_k^C, x_{k+1}^C)\phi^{\mathrm{II}}(x_k^C, x_k^b, x_k^e),$$

with $\phi^{\mathrm{I,II}}$ defined in (11). From this, taking into account the equalities

$$\overset{1}{\psi}_k + \overset{2}{\psi}_k + \overset{3}{\psi}_k = 1, \quad 1 \leqslant k \leqslant K-1,$$

we obtain the following relationships

$$\delta_k^n \leqslant \sum_{m=1}^{K-1} \lambda_{k,m}^n \delta_m^0 \leqslant \Delta^0 \sum_{m=1}^{K-1} \lambda_{k,m}^n \leqslant \Lambda_k^n \Delta^0,$$

with

$$\Lambda_k^n \leqslant 1.$$

Next, using the inequalities

$$\overset{1}{\psi}_k \leqslant \tfrac{1}{4}\Phi^2, \quad \overset{2}{\psi}_k \leqslant \Phi,$$

where

$$\Phi = 2 \max_{1 \leqslant k \leqslant K-1} \phi^{\mathrm{I}}(x_k^C, x_k^b, x_k^e),$$

we can refine the above estimates:

$$\Lambda_k^n \leqslant \begin{cases} 1, & n < K-k, \\ [(K-k)\Phi]^{n-(K-k)+1}, & n \geqslant K-k. \end{cases}$$

Hence, we finally conclude that

$$\Delta^n \leqslant q^{n-K+2}\Delta^0, \quad n \geqslant K-1, \quad q < (K-1)\Phi.$$

The required estimate for q follows immediately from the exact expressions for ϕ^{I} (see (12)):

$$\Phi \leqslant 2\frac{\exp(-\varepsilon^{-1}d^x) - \exp(-2\varepsilon^{-1}d^x)}{1 - \exp(-2\varepsilon^{-1}d^x)} \leqslant 2\exp(-\varepsilon^{-1}d^x)\exp[-\exp(-\varepsilon^{-1}d^x)\ln(2)].$$

This completes the proof of the theorem. □

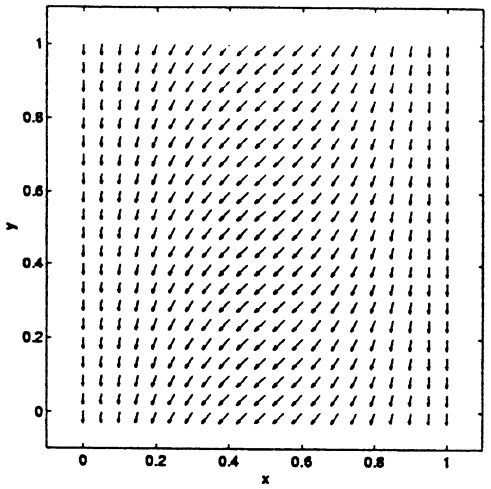


Fig. 3. Velocity field for Flow I (note: $(v^x, v^y) = (-b^x, -b^y)$).

3. Computer realization of the Schwarz methods

In this section, we consider the computer realization of the Schwarz methods. As test problems, we consider problem (1) on unit square $\Omega = (0,1) \times (0,1)$ with

$$f(P,u) = \exp[-u_0(x)] - \exp[-u(P)];\ U(P) = \begin{cases} u_0(x), & P \in \{(x,y) : \partial\Omega | y = 0\}, \\ 0, & \text{otherwise}, \end{cases} \tag{14}$$

$$u_0(x) = \sin(\pi x),$$

and with two convection vectors, called as Flow I and Flow II, respectively (see Figs. 3 and 5):

$$\text{Flow I:} \quad \boldsymbol{b}(P) = (\sin^2(\pi x),\ 1), \tag{15}$$

$$\text{Flow } II\text{:} \quad \boldsymbol{b}(P) = (\sin(2\pi x)\cos(\pi y),\ 1). \tag{16}$$

Note that both flow have constant y-component. x-component of Flow I is always positive in Ω, while Flow II changes sign at $x = \frac{1}{2}$ and $y = \frac{1}{2}$. The exact solutions of both test problems exhibit a boundary layer near the boundary $\{(x,y) : \partial\Omega | y = 0\}$. Examples of the numerical solutions of the problems (1), (14) for Flows I and II are given in Figs. 4 and 6, respectively.

Next, we describe the numerical technique used for the computer realization of the Schwarz methods.

3.1. Numerical solution scheme for the subproblems

In our experiments, we apply the following numerical approach for solving the semilinear singularly perturbed subproblems from (2) to (6): On the domain Ω, a special nonequidistant mesh Ω_h is introduced (see Section 3.2). The construction of the mesh rests on the estimates of derivatives of the exact solution of the problems (1), (14)–(16), that is, on the existence of the boundary layer

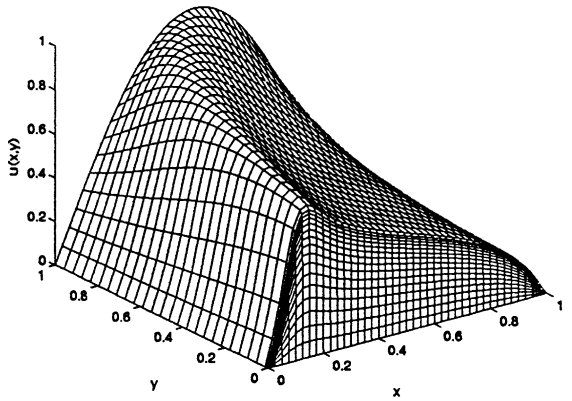


Fig. 4. Numerical solution of the test problem (1), (14), (15) at $\varepsilon = 10^{-3}$.

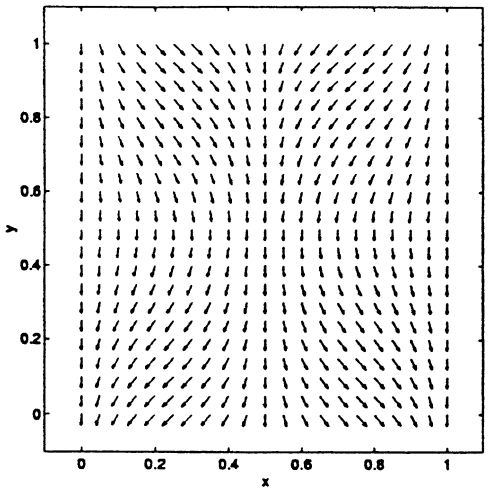


Fig. 5. Velocity field for flow (16) (see also the note for Fig. 3).

near the boundary $\{(x, y) : \partial\Omega | y = 0\}$. Domain decomposition is made compatibly with the mesh Ω_h (see Section 3.3). The subproblems are then discretized by finite differences: the diffusion part of the differential operator $\mathscr{L}$ from (1) is approximated by the five-point scheme and the convection term by the standard upwind scheme (in the case of the NDS-method, the Neumann conditions from (7) are approximated by the upwind scheme, too). For the resulting semilinear finite-dimensional subproblems, we apply the Newton's method (see, e.g., [16]). Finally, the linearized finite-dimensional subproblems are solved exactly by a factorization method (see Section 3.4 for details). We use the direct method to avoid an influence of the convergence properties of any iterative solver on experimental convergence results for the Schwarz methods.

Remark 3. As in [24,27], in order to reduce the total computational cost of the numerical realization of the Schwarz methods, we here use an inexact variant of the Newton's method: on each iteration

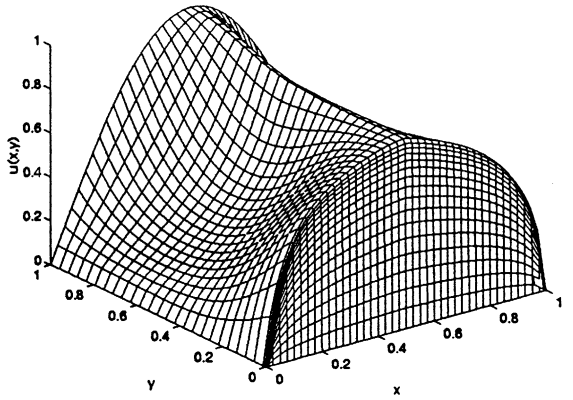


Fig. 6. Numerical solution of the test problem (1), (14), (15) at $\varepsilon = 10^{-3}$.

step of a Schwarz method only one iteration of the Newton's method is performed. Note that these realizations of the Schwarz methods are identical with realizations of the methods in which the semilinear equations in (2)–(6) are replaced by the linearized equations in the following form:

$$\mathscr{L}z^n(P) - f_u(P, z^{n-1})z^n(P) = f(P, z^{n-1}) - f_u(P, z^{n-1})z^{n-1}(P), \tag{17}$$

where f_u was defined in Section 1.

3.2. Mesh domain

We next consider the mesh generation procedure. The computational mesh for the domain $\Omega = (0,1) \times (0,1)$ is introduced by

$$\bar{\Omega}_h = \left\{ x_i = \frac{i-1}{I-1},\ 1 \leqslant i \leqslant I \right\} \times \left\{ y_j = \eta\left(\frac{j-1}{J-1}\right),\ 1 \leqslant j \leqslant J \right\}, \tag{18}$$

where I and J are the numbers of mesh points in x- and y-directions, respectively. Thus, the mesh Ω_h is uniform in x-direction (with the step size $H^x = 1/(I-1)$) and non-equidistant in y-direction with the mesh generating function $\eta(t)$ chosen in the following form [2]:

$$\eta(t) = \begin{cases} \chi(t) = -2\varepsilon \ln\left(1 - 2\dfrac{t}{\tau}\right), & t \in [0, t_*], \\ \chi(t_*) + (t - t_*) \left.\dfrac{\mathrm{d}\chi(t)}{\mathrm{d}t}\right|_{t=t_*}, & t \in [t_*, 1], \end{cases} \tag{19}$$

where $0 < t_* < \frac{1}{2}\tau$ is the root of the equation $(1-t_*)(\mathrm{d}/\mathrm{d}t)\chi(t)|_{t=t_*} = 1 - \chi(t_*)$. In (19), the parameter $0 < \tau < 1$ determines the distribution of the mesh points between the boundary layer and other part of the domain Ω. The number of the mesh points located in the boundary layer is defined by

$$J_\varepsilon = \lfloor (J-1)t_* \rfloor + 1.$$

In Figs. 4 and 6, we present examples of the approximate solutions of the test problems (1), (14) for Flows I and II, respectively, on a mesh of the form (18).

Remark 4. We emphasize that at $t \in [(J_\varepsilon - 1)/(J-1), 1]$ the mesh generating function $\eta(t)$ produces the uniform mesh with the step size H^y. From (19), it follows that H^y is a decreasing function of ε and at $\varepsilon \to 0$ we have $H^y \to 1/(J-1)(1-\tau)$.

3.3. Domain decomposition

As outlined in Section 3.1, in our experiments the domain Ω is partitioned into subdomains compatibly with the mesh Ω_h. We here use the notations introduced in Section 2.

For the mdS-method, the following subdomain partitioning is used:

$$\begin{aligned} &x_1^B = 0,\ x_k^E = x_{v_k^x + \lfloor \frac{\kappa}{2} \rfloor}, \quad x_{k+1}^B = x_{v_k^x - \lfloor \frac{\kappa+1}{2} \rfloor}, \quad x_K^E = 1, \quad 1 \leqslant k \leqslant K-1, \\ &y_1^B = 0,\ y_l^E = y_{v_l^y + \lfloor \frac{\kappa}{2} \rfloor}, \quad y_{l+1}^B = y_{v_l^y - \lfloor \frac{\kappa+1}{2} \rfloor}, \quad y_L^E = 1, \quad 1 \leqslant l \leqslant L-1, \end{aligned} \tag{20}$$

where

$$1 \leqslant \kappa \leqslant \kappa_{\mathrm{mdS}}^{\mathrm{top}} = \min[\tfrac{1}{2}(v_1^x - 1),\ \tfrac{1}{2}(v_1^y - 1),\ 2(v_1^y - J_\varepsilon)],$$

and where J_ε is the number of mesh points located in the boundary layer (Section 3.2), and

$$v_k^x = \frac{I-1}{K}k + 1, \quad 1 \leqslant k \leqslant K-1, \quad v_l^y = \frac{J-1}{L}l + 1, \quad 1 \leqslant l \leqslant L-1.$$

For the DDS- and NDS-methods, we choose the first-level subdomains $\Theta_{k,l}$ in the following way:

$$\begin{aligned} &x_0^C = 0, \quad x_k^C = x_{v_k^x}, \quad x_K^C = 1, \quad 1 \leqslant k \leqslant K-1, \\ &y_0^C = 0, \quad y_l^C = y_{v_l^y}, \quad y_L^C = 1, \quad 1 \leqslant l \leqslant L-1, \end{aligned} \tag{21}$$

while the second-level subdomains θ_k^x and θ_l^y are determined by

$$\begin{aligned} &x_k^b = x_{v_k^x - \kappa}, \quad x_k^e = x_{v_k^x + \kappa}, \quad 1 \leqslant k \leqslant K-1, \\ &y_l^b = y_{v_l^y - \kappa}, \quad y_l^e = y_{v_l^y + \kappa}, \quad 1 \leqslant l \leqslant L-1, \end{aligned} \tag{22}$$

and

$$1 \leqslant \kappa \leqslant \kappa_{\mathrm{DDS,NDS}}^{\mathrm{top}} = \min[\tfrac{1}{2}(v_1^x - 1),\ \tfrac{1}{2}(v_1^y - 1),\ v_1^y - J_\varepsilon].$$

From (20)–(22), it follows that the mesh points numbers in the subdomains $\Omega_{k,l}$ are approximately equal and those in the subdomains $\Theta_{k,l}$ are exactly equal. Moreover, in this domain decomposition, the overlapping size of the multi-domain partitioning (for the mdS-method) as well as the size of the second-level subdomains (for the DDS- and NDS-methods) are measured by a number κ of the uniform step sizes H^x and H^y (see Section 3.2):

$$\begin{aligned} &D^x = x_{v_k^x + \lfloor \frac{\kappa}{2} \rfloor} - x_{v_k^x - \lfloor \frac{\kappa+1}{2} \rfloor} = \kappa H^x, \qquad D^y = y_{v_l^y + \lfloor \frac{\kappa}{2} \rfloor} - y_{v_l^y - \lfloor \frac{\kappa+1}{2} \rfloor} = \kappa H^y, \\ &d^x = x_{v_k^x} - x_{v_k^x - \kappa} = x_{v_k^x + \kappa} - x_{v_k^x} = \kappa H^x, \quad d^y = y_{v_l^y} - y_{v_l^y - \kappa} = y_{v_l^y + \kappa} - y_{v_l^y} = \kappa H^y. \end{aligned}$$

Note that the proposed domain partitionings in y-direction minimize the common computational cost of the Schwarz methods so far, as they decrease the mesh points numbers placed in the overlapping regions.

3.4. Factorization method for the finite-dimensional subproblems

Here, we describe a direct method for solving of the finite-dimensional subproblems resulting from the application of the above discretization technique applied to a differential problem of the form (17). Any of these subproblems can be presented as a system of linear algebraic equations

$$\alpha^x_{i,j} z_{i-1,j} + \beta^x_{i,j} z_{i+1,j} + \alpha^y_{i,j} z_{i,j-1} + \beta^y_{i,j} z_{i,j+1} - c_{i,j} z_{i,j} = g_{i,j},$$
$$2 \leqslant i \leqslant m-1,\ 2 \leqslant j \leqslant M-1. \tag{23}$$

The system supplemented with boundary conditions can be written in the following 3×3-block form:

$$\begin{aligned} &-C_j Z_j + B_j Z_{j+1} = G_j,\ j = 1,\\ &A_j Z_{j-1} - C_j Z_j + B_j Z_{j+1} = G_j,\ 2 \leqslant j \leqslant M-1,\\ &A_j Z_{j-1} - C_j Z_j = G_j,\ j = M, \end{aligned} \tag{24}$$

where the blocks A_j, B_j and C_j are $m \times m$-matrices

$$A_j = \operatorname{diag}\{\alpha^y_{i,j}\}, \quad B_j = \operatorname{diag}\{\beta^y_{i,j}\}, \quad C_j = \operatorname{tridiag}[-\alpha^x_{i,j}, c_{i,j}, -\beta^x_{i,j}],$$

$Z_j = (z_{i,j}) \in \mathbb{R}^m$ are the solution blocks, and $G_j = (g_{i,j}) \in \mathbb{R}^m$ are the right-hand vectors.

For solving the above finite-dimensional problem, we use a factorization method (see, e.g., [21]), where the solution blocks are computed by the following recurrent formulae:

$$Z_j = R_{j+1} Z_{j+1} + S_{j+1}, \quad j = M-1, M-2, \ldots, 1, \qquad Z_M = S_{M+1}, \tag{25}$$

where the matrices $R_j \in \mathbb{R}^{m \times m}$ and the vectors $S_j \in \mathbb{R}^m$ are determined by

$$\begin{aligned} &R_{j+1} = Q_j B_j, \quad S_{j+1} = Q_j (A_j S_j - G_j), \quad Q_j = (C_j - A_j R_j)^{-1}, \quad j = 2, 3, \ldots, M-1,\\ &R_2 = C_1^{-1} B_1, \quad S_2 = -C_1^{-1} G_1. \end{aligned} \tag{26}$$

The total arithmetical complexity of the factorization method (24)–(26) is $\mathcal{O}(m^3 M + m^2 M)$: the calculation of the matrices Q_j, R_j and the vectors S_j, Z_j involves $\mathcal{O}(m^3 M)$ and $\mathcal{O}(m^2 M)$ operations, respectively. Thus, at $m > M$ the realization of the factorization method must be used in which i- and j-directions are interchanged in relation to the above realization.

In view of (17), the coefficients $c_{i,j}$ and the right-hand sides $g_{i,j}$ in (23) are dependent on the solution from the previous iteration step. Hence, the matrices Q_j, R_j and the vectors S_j need to be calculated anew on each iteration of the Schwarz methods.

3.5. Parallelization using MPI

Parallel implementation of the proposed Schwarz methods is based on the Message Passing Interface (MPI) library [14,27]. The DDS- and NDS-methods are realized on $K \times L$ processors as described in Remark 2. Parallel realization of the mdS-method is done using $\lfloor \frac{1}{2}(K \times L + 1) \rfloor$ processors (see Remark 1 for details).

Table 1
ε-dependence of mesh parameters

ε	10^{-1}	10^{-2}	10^{-3}	10^{-4}	10^{-5}	10^{-6}
J_ε	28	47	48	48	48	48
H^y ($\times 10^{-2}$)	0.913	1.267	1.370	1.386	1.389	1.389

4. Numerical experiments

We here report on the computational experiments for the test problems (1), (14)–(16) carried out on a distributed memory multiprocessor computer Cray T3E using the numerical approach from Section 3.1. First, we list the user-defined parameters (Section 4.1). In Section 4.2, we present experimental results for the Schwarz methods. In Section 4.3, we confront experimental convergence results with the convergence theory. Ibidem, we discuss parallel efficiency of the Schwarz methods. The Schwarz methods are compared among themselves as well as to the sequential method, that is, to the algorithm, where the test problems are solved numerically by the technique proposed to solve the subproblems (see Section 3.1).

4.1. User-defined parameters

In our experiments, we use the mesh (18) with the parameter $\tau = 0.4$ and $I = J = 121$ (i.e., $H^x = 1/(I-1) \approx 8.333 \times 10^{-3}$). The tolerance for the Schwarz methods is chosen to be 10^{-5}. The initial guesses for the methods are always taken to be zero.

We examine the Schwarz methods with different values of the critical parameters: the perturbation parameter ε, the overlapping interval sizes measured by the number κ of the uniform step sizes H^x and H^y (see Sections 3.2 and 3.3), and the partitioning numbers K and L. In experiments, we restrict the variation of κ to the following range: $1 \leqslant \kappa \leqslant \kappa^{\text{top}}$, where κ^{top} was defined in Section 3.3, and the partitioning numbers are chosen as follows: $2 \leqslant K \leqslant 5$ and $L = 2$, unless otherwise indicated. Finally, remind that H^y is a decreasing function of ε (see Remark 4 and Table 1).

4.2. Numerical results for the Schwarz methods

In Figs. 7–10, we present the experimental convergence results for the Schwarz methods with different values of the problem parameters. Fig. 7 reports the Schwarz iterations as a function of the overlapping size, while in Fig. 8, we see the iterations numbers as a function of the diffusion term ε with Flow I.

In Figs. 9 and 10, and in Tables 2 and 3, we report on the parallel efficiency E of the Schwarz methods for Flows I and II. To provide experimental results which are independent of the numerical solution method for the subproblems (see Section 3.4) we use the following nonstandard notation for the parallel efficiency:

$$E = \frac{S}{c_{\text{cr}}\, p},$$

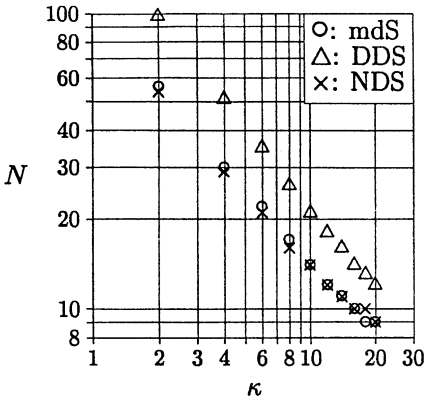


Fig. 7. Flow I: number N of Schwarz iterations as a function of the overlapping size κ with diffusion $\varepsilon = 10^{-1}$ and partitioning numbers $K = 3$ and $L = 1$.

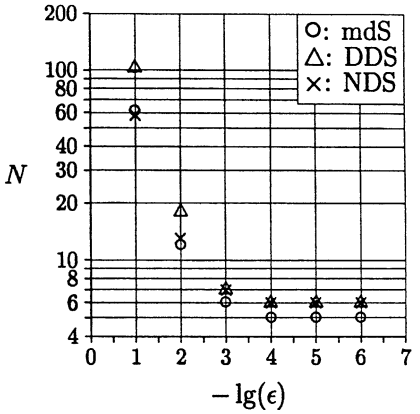


Fig. 8. Flow I: number N of Schwarz iterations as a function of the diffusion term ε with overlapping $\kappa = 2$ and partitioning numbers $K = 3$ and $L = 2$.

where $S = T_{\mathrm{sq}}/T_{\mathrm{S}}$ is the speedup for the Schwarz methods with respect to the sequential method (T_{sq} is the execution time for the sequential method and T_{S} for the parallel Schwarz methods), p is the number of the processors used in parallel ($p = \frac{1}{2}K \times L$ for the mdS-method or $p = K \times L$ for the DDS- and NDS-methods), and $c_{\mathrm{cr}} = K^2$ is the *correction coefficient* which allows for the nonlinear dependence of the computational cost of the factorization method for the "big" subproblems (the subproblems related to the subdomains $\Omega_{k,l}$ or $\Theta_{k,l}$) on the dimensions of these subproblems (remind that at $K \geqslant L$ the mentioned computational cost behaves like $\mathcal{O}(K^{-3}L^{-1})$, see Sections 3.4 and 3.3). The figures demonstrate the κ-dependence of E for the Schwarz methods with different ε and the partitioning number K. In the tables, we present the maximum values of the parallel efficiency for the methods:

$$E^{\max} = \max_{1 \leqslant \kappa \leqslant \kappa^{\mathrm{top}}} E(\kappa) = E(\kappa^{\mathrm{opt}}), \quad \varepsilon,\ K \text{ and } L \text{ are fixed.}$$

The values of κ^{opt} and the required iterations number $N^{\mathrm{rq}} = N(\kappa^{\mathrm{opt}})$ are also listed in the tables.

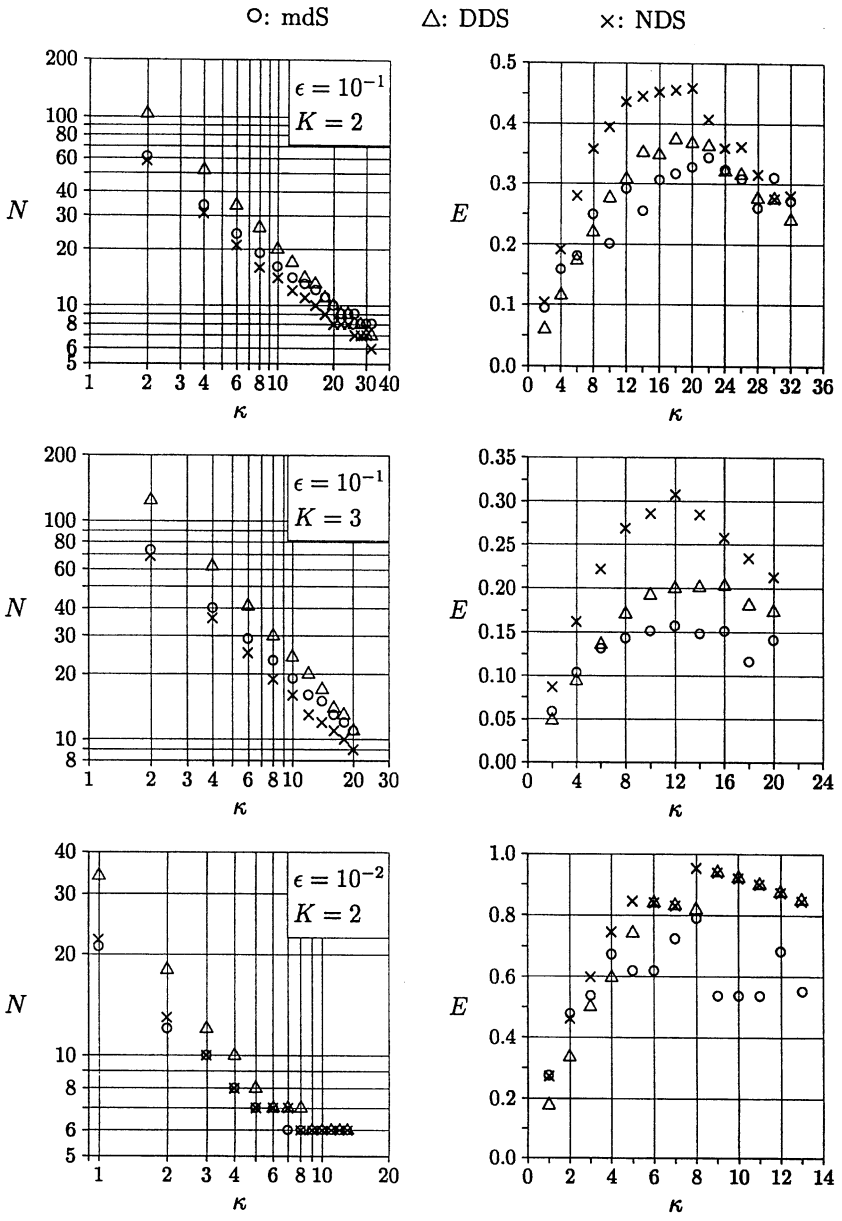


Fig. 9. Flow I: number N of Schwarz iterations and the parallel efficiency E as a function of the overlapping size κ for different diffusions ε and partitioning number K $(L = 2)$.

4.3. Discussion of numerical results

4.3.1. Flow I

First, we dwell on the convergence properties of the Schwarz methods. Figs. 7–9 show that the iterations number N for the Schwarz methods is an increasing function of the perturbation parameter

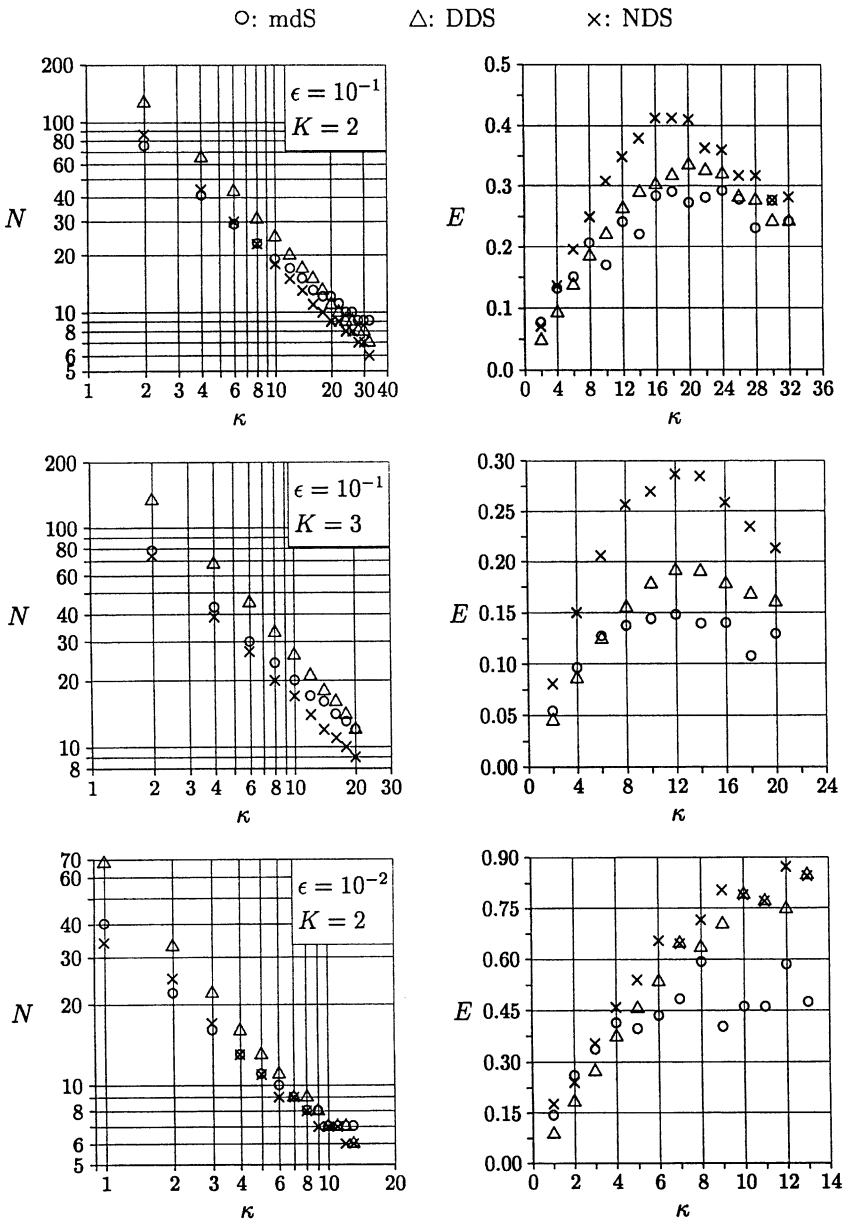


Fig. 10. Flow II: number N of Schwarz iterations and the parallel efficiency E as a function of the overlapping size κ for different diffusions ε and partitioning number K ($L = 2$).

ε and a decreasing function of the overlapping interval sizes (measured by the number κ). As the data of Fig. 9 suggest, at fixed ε and L, the number of iterations is an increasing function of K. Note that these numerical results are in qualitative agreement with the theoretical estimate obtained for the model problem (1), (8) in the case of a strip domain decomposition with $L = 1$ (see Theorem 1).

Table 2
Flow I: maximum values of the parallel efficiency $E^{\max}$, the related overlapping values κ^{opt} and the required number N^{rq} of Schwarz iterations for different diffusion terms ε and partitioning numbers K $(L=2)$[a]

K	$E^{\max}$, κ^{opt}, N^{rq}																	
2	0.34	22	9	0.79	8	6	0.95	2	6	1.09	2	5	1.14	1	5	1.14	1	5	m
3	0.16	12	16	0.48	6	8	0.60	2	7	0.79	1	7	0.92	1	6	0.92	1	6	d
4	0.12	10	20	0.37	7	8	0.60	3	7	0.74	1	7	0.87	1	6	0.87	1	6	S
5	0.09	8	27	0.31	6	9	0.49	4	7	0.61	2	7	0.69	1	7	0.68	1	7	
2	0.37	18	11	0.94	9	6	1.00	3	6	1.00	2	6	1.00	1	6	1.00	1	6	D
3	0.21	15	15	0.66	10	7	0.85	3	7	0.85	2	7	0.86	1	7	0.86	1	7	D
4	0.13	10	26	0.46	8	9	0.68	4	8	0.72	2	8	0.73	1	8	0.73	1	8	S
5	0.09	9	32	0.34	5	13	0.56	3	9	0.58	2	9	0.59	1	9	0.59	1	9	
2	0.48	17	9	0.95	8	6	1.00	3	6	1.00	3	6	1.00	1	6	1.00	1	6	N
3	0.31	12	13	0.70	9	7	0.85	3	7	0.85	2	7	0.86	1	7	0.86	1	7	D
4	0.20	10	17	0.52	5	10	0.71	3	8	0.72	2	8	0.73	1	8	0.73	1	8	S
5	0.14	7	26	0.40	5	11	0.56	3	9	0.59	2	9	0.59	1	9	0.59	1	9	
ε	10^{-1}			10^{-2}			10^{-3}			10^{-4}			10^{-5}			10^{-6}			
N_{sq}	4			4			4			4			4			4			

[a] N_{sq} is the number of Newton's iterations required for solving the test problem by the sequential method. The ε-dependence of N_{sq} is appended for reference.

At $N \gg N_0$, Theorem 1 predicts the proximity of the convergence rate for the mdS-method with that for the NDS-method. Fig. 7 confirms the theoretical result at $L=1$. However, the experimental results presented in Fig. 9 show that in the case of the "box" domain decomposition (i.e., with $K,L>1$) and at $\varepsilon=10^{-1}$ the iterations number N for the mdS-method is slightly bigger than the corresponding values of N for the NDS-method. As expected from Theorem 1, the experimental convergence rate for the DDS-method is noticeably smaller than that for the mdS- and NDS-methods (see Figs. 7 and 9).

From Theorem 1, one would expect that the minimum value of the required Schwarz iterations equals N_0 with $N_0=\lfloor \frac{1}{2}K \rfloor$ for the mdS-method and $N_0=K-1$ for the DDS- and NDS-methods. From Table 2 (see also Fig. 8), it follows that at $\varepsilon \leqslant 10^{-5}$, the required iterations numbers are close to N_0+N_{sq}, where N_{sq} is the numbers of Newton's iterations required for solving the original test problem by the sequential method. This is explained by using the inexact variant of the Newton's method for solving the semilinear subproblems (see Remark 3).

Next, we discuss some common issues related to the parallel efficiency of the Schwarz methods. Evidently, the positions (κ^{opt}) and the magnitudes of the parallel efficiency maxima ($E^{\max}$) are determined by two opposite processes associated with rise of κ, at fixed ε and K: the decreasing the number N of iterations and the increasing the number of mesh points in overlapping regions. Thus, the greater is the value of $N(1)-N(\kappa^{\text{top}})$, the greater is the value of κ^{opt}, and the less is the maximum values of the parallel efficiency $E^{\max}$ (see Fig. 9). Hence, the dependence of κ^{opt} and $E^{\max}$ on the diffusion term ε as well as the partitioning number K (see Table 2) is explained by the

Table 3
Flow II: maximum values of the parallel efficiency $E^{\max}$, the related overlapping values κ^{opt} and the required number N^{rq} of Schwarz iterations for different diffusion terms ε and partitioning numbers K $(L = 2)$[a]

K	$E^{\max}$, κ^{opt}, N^{rq}																	
2	0.29	23	10	0.59	8	8	0.77	4	7	0.93	2	6	0.93	2	6	0.93	2	6	m
3	0.15	13	16	0.45	7	8	0.59	3	7	0.79	1	7	0.92	1	6	0.92	1	6	d
4	0.11	10	22	0.34	8	8	0.55	4	7	0.79	2	6	0.87	1	6	0.87	1	6	S
5	0.08	8	29	0.31	6	9	0.55	3	7	0.61	2	7	0.71	2	6	0.71	2	6	
2	0.34	20	11	0.85	13	6	0.99	5	6	1.00	3	6	1.00	2	6	1.00	2	6	D
3	0.20	13	19	0.65	10	7	0.84	3	7	0.85	2	7	0.86	1	7	0.86	1	7	D
4	0.12	10	29	0.48	9	8	0.78	4	7	0.83	2	7	0.83	1	7	0.83	1	7	S
5	0.08	7	47	0.36	7	10	0.56	3	9	0.62	3	8	0.65	2	8	0.63	2	8	
2	0.41	16	11	0.87	12	6	0.99	5	6	1.00	3	6	1.00	2	6	1.00	1	6	N
3	0.29	11	15	0.73	8	7	0.85	3	7	0.85	2	7	0.86	1	7	0.85	1	7	D
4	0.17	8	25	0.52	8	8	0.78	4	7	0.82	2	7	0.83	1	7	0.83	1	7	S
5	0.13	7	28	0.44	5	10	0.58	4	8	0.62	3	8	0.64	2	8	0.64	2	8	
ε	10^{-1}			10^{-2}			10^{-3}			10^{-4}			10^{-5}			10^{-6}			
N_{sq}	4			4			4			4			4			4			

[a] N_{sq} is the number of Newton's iterations required for solving the test problem by the sequential method. The ε-dependence of N_{sq} is appended for reference.

corresponding dependence of N on these "critical" parameters. It should be noted that an additional reason for the K-dependence of $E^{\max}$ is the degradation of the relation between the sizes (measured as the number of the mesh nodes) of the overlapping regions and those of the "big" subdomains (the subdomains $\Omega_{k,l}$ for the MDS-method or $\Theta_{k,l}$ for the DDS- and NDS-methods) with increasing K at fixed κ.

Remark 5. In the case of the mdS-method, the existence of "peaks" and "pits" on the "curves" $E(\kappa)$ (Fig. 9) as well as the "superefficiency" of the method (i.e., $E^{\max} > 1$), at $\varepsilon \leqslant 10^{-4}$ and $K = 2$, are a result of the cache-memory effect (see [27,26] for details).

As is clear from Table 2, at $\varepsilon \geqslant 10^{-2}$, the parallel implementation of the NDS-method is faster than that of the DDS-method and at $\varepsilon \leqslant 10^{-3}$ these methods have the identical parallel efficiency. At $\varepsilon \geqslant 10^{-3}$, the mdS-method is exceeded in the parallel efficiency even by the DDS-method. But at $\varepsilon \leqslant 10^{-5}$ and for all values of K, the mdS-method is slightly faster than both the two-level Schwarz methods, because then the convergence properties of the Schwarz methods are dictated by the value of N_0 which is smallest for the first method.

4.3.2. Flow II

Here, we shortly discuss experimental results for the test problem Flow II. Recall that Flow II differs from Flow I in x-component (it is always positive for Flow I and changes sign at $x = \frac{1}{2}$

and $y = \frac{1}{2}$ for Flow II). The juxtaposition of the data from Figs. 9 and 10 indicates that at $K = 2$ (when a substantial part of the overlapping regions is placed in the zone near $x = \frac{1}{2}$) the convergence rates of the Schwarz methods in the case Flow II are noticeable less than in Flow I. At $K = 3$, the overlapping regions are some distance away from the zones where x-component of the transport vector changes sign. In this case, the convergence properties of the Schwarz methods are close to those for Flow I (cf., Figs. 9 and 10 and Tables 2 and 3). Moreover, we note that, at fixed ε and given κ, changing K from 2 to 3 leads to even a reduction in the number of iterations for the NDS-method. This "anomalous" behaviour of the NDS-method can be explained by the fact that at $K = 3$ the boundary conditions of Neumann-type are applied to bigger part of the boundaries of the two-level subdomains θ_k^x than at $K = 2$ (see (7) and (16)).

5. Conclusions

We have compared the parallel implementation of the three variants of the Schwarz method: the multi-domain generalization of the standard Schwarz alternating method, the two-level Schwarz method with interface subproblems and its modification (the method with a combination of Dirichlet and Neumann boundary conditions for interface subproblems). The experimental results obtained for two test problems substantiate a priori estimates of the convergence rates for the Schwarz methods with respect to the diffusion term ε, the overlapping interval sizes, and the number of the domain partitioning. It has been demonstrated that for the test problems, at $10^{-2} \leqslant \varepsilon \leqslant 10^{-1}$, the parallel efficiency of the modified two-level Schwarz method is superior to that of two other examined methods. At $\varepsilon \leqslant 10^{-4}$, the parallel efficiencies of all considered methods are close to each other.

Acknowledgements

Matter Research was done during the first author's visits at the Department of Mathematical Information Technology of the University of Jyväskylä (September–November, 1998 and October–November, 1999); the visits were supported by the Academy of Finland and the University of Jyväskylä. The numerical experiments were carried out on a Cray T3E computer, located in Center for Scientific Computing, Espoo, Finland.

References

[1] M. Allen III, I. Herrera, G. Pinder, Numerical Modeling in Science and Engineering, Wiley-Interscience, New York, 1988.
[2] N. Bakhvalov, On optimization of methods for solving boundary value problems in the presence of boundary layers, Zh. Vychisl. Mat. Mat. Fiz. 9 (1969) 841–859 (in Russian).
[3] I. Boglaev, V. Sirotkin, Numerical solution of quasi-linear singularly perturbed heat-conduction equations on non-uniform grids, USSR Comput. Math. Math. Phys. 30 (1990) 28–40.
[4] I. Boglaev, V. Sirotkin, Domain decomposition technique for singularly perturbed problems and its parallel implementation, in: J. Miller, R. Vichenevetsky (Eds.), Proceedings of the 13th IMACS World Congress on Computation and Applied Mathematics, IMACS, Dublin, 1991, pp. 522–523.
[5] X. Cai, W. Gropp, D. Keyes, A comparison of some domain decomposition and ILU preconditioned iterative methods for nonsymmetric elliptic problems, Numer. Linear Algebra Appl. 1 (1994) 477–504.

[6] X. Cai, M. Sarkis, Local multiplicative Schwarz algorithms for steady and unsteady convection–diffusion equations, East-West J. Numer. Math. 6 (1998) 27–41.
[7] T. Chan, T. Mathew, Domain decomposition preconditioners for convection diffusion problems, in: Y. Kuznetsov et al. (Eds.), Domain Decomposition Methods in Science and Engineering, AMS, Philadelphia, 1994, pp. 157–175.
[8] M. Garbey, A Schwarz alternating procedure for singular perturbation problems, SIAM J. Sci. Comput. 17 (1996) 1175–1201.
[9] V. Giovangigli, M. Smooke, Calculation of extinction limits for premixed laminar flames in a stagnation point flow, J. Comput. Phys. 68 (1987) 327–345.
[10] G. Hedstrom, F. Howes, A domain decomposition method for a convection diffusion equation with turning point, in: T. Chan et al. (Eds.), Domain Decomposition Methods, SIAM, Philadelphia, 1989, pp. 38–46.
[11] Y. Kuznetsov, Overlapping domain decomposition methods for FE-problems with elliptic singular perturbed operators, in: R. Glowinski et al. (Eds.), Fourth International Symposium on Domain Decomposition Methods for Partial Differential Equations, SIAM, Philadelphia, 1991, pp. 223–241.
[12] O. Ladyzhenskaya, N. Ural'tseva, Linear and Quasilinear Elliptic Equations, Academic Press, New York, 1968.
[13] T. Mathew, Uniform convergence of the Schwarz alternating method for solving singularly perturbed advection–diffusion equations, SIAM J. Numer. Anal. 35 (1998) 1663–1683.
[14] Message Passing Interface Forum, MPI: a message-passing interface standard, Technical Report CS-94-230, Computer Science Department, University of Tennessee, 1994.
[15] E. O'Riordan, M. Stynes, A globally uniformly convergent finite element method for a singularly perturbed elliptic problem in two dimensions, Math. Comp. 57 (1991) 47–62.
[16] J. Ortega, W. Rheinboldt, Iterative Solution of Nonlinear Equations in Several Variables, Academic Press, New York, 1970.
[17] L. Pouly, J. Pousin, Modeling and numerical investigation of a droplets combustion problem, in: C. Hirsch et al. (Eds.), First European Conference on Numerical Methods in Engineering, Elsevier, Amsterdam, 1992, pp. 851–857.
[18] L. Pouly, J. Pousin, A spray combustion problem, Math. Models Methods Appl. Sci. 2 (1994) 237–249.
[19] G. Rodrigue, E. Reiter, A domain decomposition method for boundary layer problems, in: T. Chan et al. (Eds.), Domain Decomposition Methods, SIAM, Philadelphia, 1989, pp. 226–234.
[20] F. Rothe, Global Solutions of Reaction-Diffusion Systems, Springer, New York, 1984.
[21] A. Samarskii, Theory of Finite Difference Schemes, Nauka, Moscow, 1989 (in Russian).
[22] H. Schwarz, Über einige Abbildungsaufgaben, Ges. Math. Abh. 11 (1869) 65–83.
[23] S. Selberherr, Analysis and Simulation of Semiconductor Devices, Springer, New York, 1984.
[24] V. Sirotkin, Solution of singularly perturbed semilinear elliptic problem by iterative domain decomposition algorithms, Comput. Math. Appl. 33 (1997) 99–116.
[25] V. Sirotkin, Solution of singularly perturbed elliptic problems by a two-level parallel Schwarz algorithm using a "Neumann–Dirichlet" scheme, Appl. Numer. Math., submitted for publication.
[26] V. Sirotkin, P. Tarvainen, Parallel two-level Schwarz methods for singularly perturbed elliptic problems, Numer. Algorithms 22 (1999) 129–156.
[27] V. Sirotkin, P. Tarvainen, Overlapping Schwarz methods for a singularly perturbed semilinear elliptic problem and their parallel implementation, SIAM J. Sci. Comp. 21 (2000) 1587–1608.